IAC-17.A6.3.6x41656

CHARACTERIZING DEBRISAT FRAGMENTS: SO MANY FRAGMENTS, SO MUCH DATA, AND SO LITTLE TIME

B. Shiotani, M. Rivero, M. Carrasquilla, S. Allen[1]

N. Fitz-Coy[1], J.-C. Liou[2], T. Huynh[3], M. Sorge[4], H. Cowardin[5], J. Opiela[6], and P. Krisko[6]

[1]The University of Florida, USA, [2]National Aeronautics and Space Administration, USA, [3]United States Air Force/Space and Missile Systems Center, USA, [4]The Aerospace Corporation, USA, [5]University of Texas at El Paso - Jacobs JETS Contract, NASA Johnson Space Center, Houston, TX, USA, [6]Jacobs, NASA Johnson Space Center, Houston, TX, USA.

To improve prediction accuracy, the DebriSat project was conceived by NASA and DoD to update existing standard break-up models. Updating standard break-up models require detailed fragment characteristics such as physical size, material properties, bulk density, and ballistic coefficient. For the DebriSat project, a representative modern LEO spacecraft was developed and subjected to a laboratory hypervelocity impact test and all generated fragments with at least one dimension greater than 2 mm are collected, characterized and archived. Since the beginning of the characterization phase of the DebriSat project, over 130,000 fragments have been collected and approximately 250,000 fragments are expected to be collected in total, a three-fold increase over the 85,000 fragments predicted by the current break-up model. The challenge throughout the project has been to ensure the integrity and accuracy of the characteristics of each fragment. To this end, the post hypervelocity-impact test activities, which include fragment collection, extraction, and characterization, have been designed to minimize handling of the fragments. The procedures for fragment collection, extraction, and characterization were painstakingly designed and implemented to maintain the post-impact state of the fragments, thus ensuring the integrity and accuracy of the characterization data. Each process is designed to expedite the accumulation of data, however, the need for speed is restrained by the need to protect the fragments. Methods to expedite the process such as parallel processing have been explored and implemented while continuing to maintain the highest integrity and value of the data. To minimize fragment handling, automated systems have been developed and implemented. Errors due to human inputs are also minimized by the use of these automated systems.

This paper discusses the processes and challenges involved in the collection, extraction, and characterization of the fragments as well as the time required to complete the processes. The objective is to provide the orbital debris community an understanding of the scale of the effort required to generate and archive high quality data and metadata for each debris fragment 2 mm or larger generated by the DebriSat project.

I. BACKGROUND AND CURRENT STATUS

The DebriSat test article is a representative of a typical modern low Earth orbit (LEO) satellite that was subjected to a laboratory hypervelocity impact (HVI) test in April 2014 [1,2]. The overall objective of DebriSat project is to update existing standard satellite break-up models with components and materials common to modern LEO spacecraft. For the laboratory HVI test, the DebriSat test article was suspended within a "soft-catch" arena formed by polyurethane foam panels to protect the debris fragments from the metal walls of the test chamber. After the laboratory HVI test, all the foam panels and debris fragments within the test chamber were collected and transported to University of Florida for fragment processing and characterization. Since the 2014 laboratory HVI test, the DebriSat team has been collecting, extracting, characterizing, and archiving fragments down to 2 mm in length.

In order to characterize the DebriSat fragments, a rigorous process was developed and implemented. There are three major tasks associated with the post-impact processing of DebriSat fragments: detection, extraction, and characterization. Each task and its associated sub-tasks and activities are shown in Figure 1. The detection task has three sub-tasks beginning with foam panel preparation where loose fragments and fragments embedded on the surfaces of the panels are collected and stored. Once panel preparation is completed, the panels are X-ray imaged. After the X-ray images are acquired, they are post-processed to detect other embedded fragments. The extraction task involves the careful extraction of fragments with at least one dimension greater than 2 mm which are stored individually. The approximate location of each fragments on or in the panel is recorded to provide information on physical distribution and penetration depth. The fragments are recorded into the DebriSat Categorization System (DCS)

database where each fragment is given a unique identification number [3,4]. The characterization task involves fragment assessments (2D/3D size discriminator, material, shape, and color), measurements (mass and physical size X_{DIM}, Y_{DIM}, and Z_{DIM}), and the size characteristics from the measurements (i.e., determining the characteristic length, average cross-sectional area, and volume) are calculated. All the fragment data and images generated throughout the process as well as the associated metadata (revision history, creator, timestamp, etc.) are all uploaded and stored on the DCS. Once the fragments are characterized, each fragment goes through a verification process where technicians confirm the data archived in the DCS database. The fragment verification ensures the integrity of the fragment data generated throughout the post-HVI process. In addition, Gage repeatability and reproducibility (Gage R&R) tests are conducted every 1,000 verified fragments to quantify the variations in equipment and procedure. The Gage R&R tests maintain high levels of confidence in the fragment characterization data.
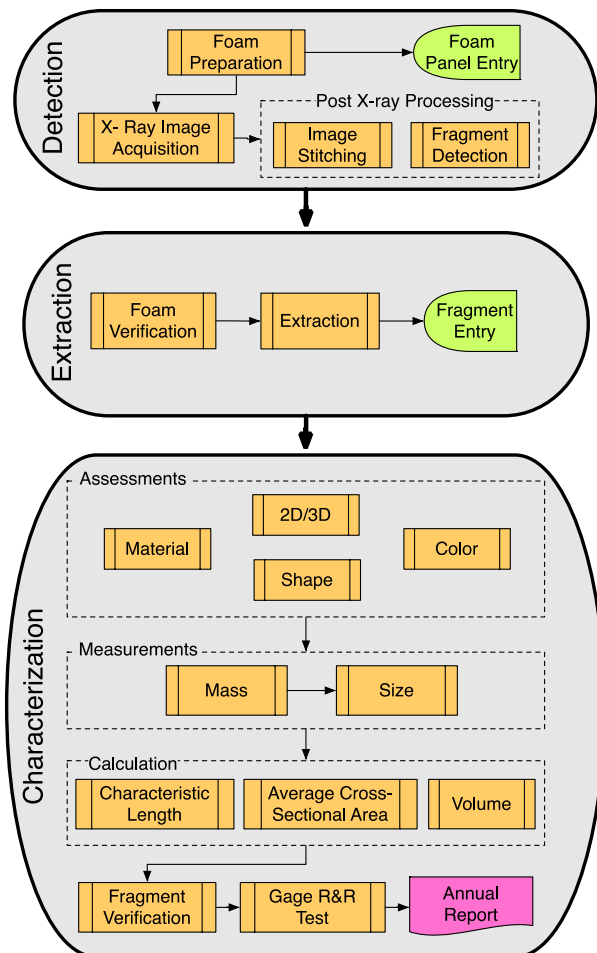

Figure 1 Post-HVI processes

A total of 588 foam panels were installed inside the test chamber during DebriSat's laboratory HVI test. Three different density panels, denoted low, medium, and high, were stacked and utilized to capture debris fragments inside the chamber. The foam panels were arranged such that the density of the panels increased radially out towards the wall of the test chamber.

Table 1 shows the progression of debris fragment processing from the post-HVI test to the present (as of August 2017). Panel preparation and recording fragments in the database were the main focus in 2014 – 2015. The focus for the 2015 – 2016 was to X-ray the foam panels, extract fragments from the foam panels, and to begin fragment characterization. The recent efforts have been focused on fragment extraction and fragment characterization, while there are steady increases in panel preparation and X-ray image acquisition. No fragments were verified in the first two years, however, there have been close to 3,000 fragments that have been verified thus far.

Table 1 Status of post-HVI processing

	2014-2015	2015-2016	2016-2017
Panels prepared	304	369	382
Panels X-rayed and post-processed	None	279	295
Panels extracted	None	62	285
Fragments collected	90,000	125,000	154,000
Fragments recorded in DCS	73,571	117,712	138,210
Fragments extracted	None	9,344	31,144
Fragments characterized	None	882	13,886
Fragments verified	None	None	2,842

As of August 2017, of the 588 panels used to construct the soft-catch arena, 382 full panels have been prepared for X-ray imaging; for compactness we denote this as 382/588 panels have been processed for X-ray imaging. Full panels are defined as panels with greater than 2/3 of its planform intact and the remaining 208/588 panels are broken into pieces smaller than 2/3 of the panels' planform. Embedded objects have been identified in 295/382 prepared panels which have been X-ray imaged and fragments have been extracted from 282/295 of the X-ray imaged panels. The processing of the 382 full panels took over 1,200 hours (i.e., 0.6 person-year) to complete, averaging approximately 3 hours per panel. The X-ray imaging of 295 panels took 150 hours to complete, averaging approximately half an hour per panel. To complete extracting fragments from 285 full panels took over 2,800 hours (i.e., 1.4 person-year), averaging 10 hours per panel. The average times to

extract fragments from medium and high density panels are less than 6 hours, however, the times for low density panels is approximately 22 hours. Since the panels were arranged in the test chamber such that the panel density increased radially outward, during the impact test majority the fragments impacted the low density panels and only the more energetic fragments reached the higher density panels (shown in Figure 2).

Table 2 Processing times per panel

	Number of panels	Total time (hr)	Average time (hr)
Panel preparation	382 / 588	1222.4	3.2
X-ray imaging	295 / 382	150.0	0.5
Extraction	282 / 295	2876.4	10.2
Low density	78	1723.8	22.1
Medium density	135	810.0	6.0
High density	69	165.6	2.4

Figure 2 Panel layout inside chamber (left) and the aftermath (right)

An initial estimate of 85,000 debris fragments were predicted by the current NASA satellite break-up model. To date, 138,210 fragments have been collected and entered into the DCS database and approximately 15,790 fragments are awaiting database entry for approximately 154,000 fragments that have been collected post-HVI testing. Over 107K fragments have been collected and recorded from panel preparations and over 31K fragments have been extracted and recorded from the extraction activities. Out of the 138,210 fragments that are archived in the DCS database, 13,886 fragments have completed characterization (assessment, mass, and size measurements) and of that 13,886 fragments, 2,842 fragments have completed verification. The fragment counts are shown in Table 3. To note, the characterization effort began with fragments that qualify as 2D (i.e., small and/or negligible thickness) and carbon fiber reinforced polymer (CFRP). Details of characterization using the 2D imaging system will be discussed in II.III. As of 2017, the effort to characterize fragments using both the 2D and 3D imaging systems in underway to extract information with more complex, sizeable fragments.

In this paper, the processes and challenges involved in the collection, extraction, and characterization of the DebriSat fragments are discussed. Each task and

activities are rigorously designed, developed, and implemented to ensure that all fragment data and associated metadata are properly captured and archived in the database. Due to the sheer number of fragments and their associated data to be captured and stored, as well as the ever changing group of technicians (undergraduate students), the post-processing of DebriSat fragments is a daunting task. However, to address these challenges, many of the processes have been automated and streamlined to increase fragment processing throughput as well as ensure independence of the technicians (i.e., minimize subjectivity) on the generated data. The processing facility layout continues to be updated to organize activities and workstations such that the post-HVI activities are streamlined. The paper is outlined as follows: details the post-HVI processes, challenges and updates implemented throughout the post-processing activities to efficiently yet at high quality, collect and archive the DebriSat fragment data.

Table 3 Number of fragments recorded in the DCS

	Number of fragments
Panel preparation	107,066
Extraction	31,144
Characterization	13,886
Verification	2,849
Total in the DCS	138,210

II. POST-HVI PROCESSES AND UPDATES

The post-HVI process is decomposed into three major tasks: detection, extraction and characterization. In this section, each task is discussed to highlight the challenges and the resolutions that were implemented.

II.I Detection

The soft catch arena installed in the chamber was constructed with 588 panels organized into three sections: up-range where the projectile entered the arena, side which protects the fragments from impacting the chamber walls, and down-range which acts as a backstop to prevent fragments from blowing downstream of the impact point. The up-range section had 24 panels installed, the side section had 452 panels, and the down-range section 112 panels. The side section was further subdivided into five rows with Row 1 closest to down-range section and Row 5 closest to up-range section. Further details of the panel distribution are shown in Table 4. Each panel was designated based on their chamber location and their placement in the panel stack, which was used to uniquely identify and archive the information in the DCS database. To date, 382 panels have been processed and prepared for X-ray image acquisition. These 382 panels are panels that are at least 2/3 of the original panel planform (referred to as full panels) and the remaining panels are all less than the 2/3 of the original panel planform (referred to as broken

panels). A procedure to prepare the full panels have been developed and implemented, and a procedure for preparing broken panels is developed and is ready to be implemented. The procedure for preparing broken panels is different from the procedure for full panels due to its smaller form. To provide all broken panels with unique identification would be prohibitively time consuming, therefore, unique foam panel IDs are only given to broken panels with a minimum length greater than 10 cm.

Table 4 Foam panels prepared

Chamber section	Panels in chamber	Panels prepared
Down range	112	43
Up range	24	18
Side	452	319
Row 1	92	84
Row 2	92	85
Row 3	92	76
Row 4	92	30
Row 5	84	44
Unknown		2
Total panel count	588	382

Of the prepared full panels, 109/382 were low density, 205/382 were medium density, and 66/382 were high density. Two of the panels were severely charred and their designations were not visible, thus, their row identifications are denoted as unknown in Table 4.

The preparation times for each panel density category are shown in Figure 3 and Table 5, specifically, the average, maximum, and minimum times required to prepare the panels are shown. The preparation times for the low density panels are significantly greater than the preparation times for medium and high density panels, since most of the fragments were captured by the low density panels.
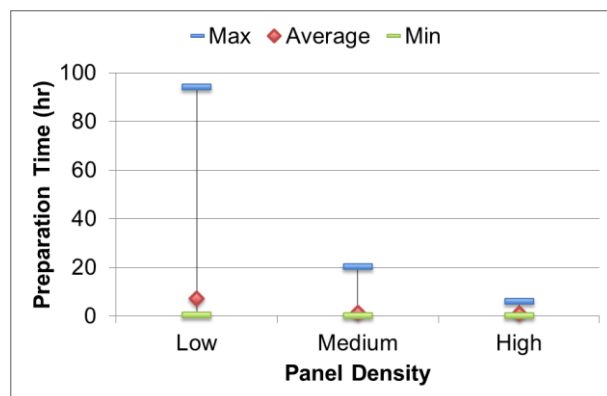

Figure 3 Full foam panel preparation times

Once the full panels were prepared, they were transported to the X-ray facility and imaged. Due to the size limitation of the X-ray detector, 12 images are required to cover the entire full panel. The X-ray images are then post-processed where they are stitched together and an object detection algorithm applied to detect embedded fragments. To date, a total of 295 full panels have been X-ray imaged and post-processed. The average X-ray image acquisition time is half an hour per panel (see Table 1) and a few minutes to post-process each set of panel X-rays. A malfunction of the X-ray equipment has caused a delay in the imaging of the remainder of the prepared panels. Once the X-ray imager is repaired and functional, the team will complete X-ray imaging of all prepared panels. X-ray imaging of broken panels will commence once all full panels have been X-ray imaged. However, rather than imaging each broken panel individually, multiple broken panels will be made into a faux panel and imaged and post-processed. A procedure to image and post-process the broken panels is currently being developed and will be verified prior to implementation. The X-ray image acquisition and post-processing times are to be analyzed once the broken panel X-ray imaging begins.

Table 5 Foam panels preparation times

Preparation time	Low	Medium	High
Panel count	109	205	66
Max (hrs)	94.2	20.4	6.2
Average (hrs)	7.2	1.4	1.0
Min (hrs)	0.5	0.2	0.2

II.II Extraction

Prior to carefully extracting the fragments identified from the post-processed X-ray images, each panel is verified to ensure that the preparation data are properly entered into the DCS database. With the panels verified, fragments with at least one dimension greater than 2 mm are carefully extracted and archived in the DCS with unique fragment identification numbers. The extraction procedure is to scrape away at the surface of the foam panels with tweezers and carving tools to excavate the debris fragments. The procedures differ slightly depending on the density of the foam panels, however, the main difference is merely the choice of tools used to excavate the fragments from the foam panels [1].

Currently, a total of 285 full panels have completed extraction, out of which 79 panels are low density, 135 panels are medium density, and 71 panels are high density. The average, maximum, and minimum extraction times for each panel density are shown in Figure 4 and Table 6. Similar to the preparation times, the low density panels require more time for extraction on average due to the higher fragment counts captured in them. There was a low density panel that took over 160 hours to complete extraction and over 3,500 fragments were collected from that panel. For some high density and medium density panels, there were no embedded fragments identified through the X-ray images, therefore,

the surfaces of the panels were carefully inspected to ensure that no fragments are captured in the panels. It should be noted that, the extraction task involves two to four technicians per panel.
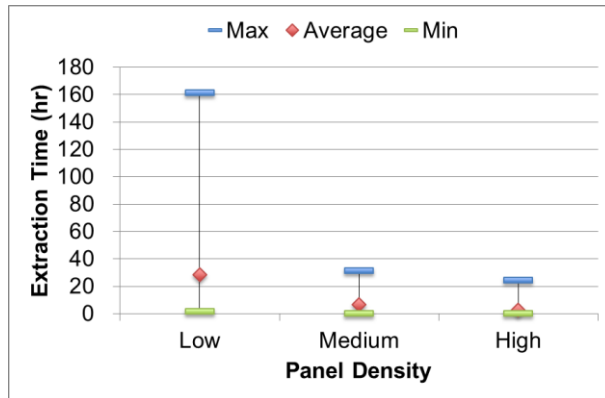

Figure 4 Foam panel extraction times

Table 6 Foam panels extraction times

Extraction time	Low	Medium	High
Panel count	79	135	71
Max (hrs)	161.3	38.8	24.3
Average (hrs)	21.9	6.0	2.3
Min (hrs)	0.8	0.2	0.1

After extraction was completed on several panels, they were re-X-ray imaged to ensure no fragments were missed during extraction. No fragments were identified in the reimaged medium and high density panels; however, several fragments were detected in some reimaged low density panels. One reason why there were some fragments detected from the post-extracted low density panels was that those panels were processed with an early version of the object detection algorithm. The early object detection algorithm had challenges in stitching the 12 X-ray images, where the fragments located in the boundaries of the images were not identified. In addition, the early algorithm filtered objects smaller than two pixels, thus, the smaller fragments were not properly identified. However, updates have been made to the object detection algorithm where the image stitching has improved to detect fragments in the boundaries and the two-pixel filter has been removed. The extracted low density panels are re-extracted to recover fragments that were missed due to the early object detection algorithm. It is anticipated that once panels that were initially processed using the updated object detection algorithm are reimaged this will no longer be an issue. However, to date, only those panels that were processed with the early version of the detection algorithm have been reimaged.

II.III Characterization

All fragments collected during preparation and extraction are individually bagged, assigned a unique fragment identification number, and entered into the DCS database. First, the panel information associated with the fragment are entered and this information provides general insights into the location of the fragment post-HVI. Next, the fragment's physical attributes are assessed and entered; the fragment's physical attributes are (i) size category (i.e., 2D or 3D fragment), (ii) material property, (iii) shape, and (iv) color. Once all assessments are completed, the fragment's mass and size are measured and entered into the DCS database along with associated metadata. Prior to finalizing the database entries associated with a fragment, an independent technician (one who has no prior involvement with the fragment) reviews and certifies that the database entries are valid; once this certification has been completed, the fragment database entry is locked and no further modifications are possible.

The initial characterization effort was focused on fragments that were categorized as 2D and these were primarily carbon fiber reinforced polymer (CFRP) fragments. This focus was based on the fact that the first size characterization system to become available was the 2D imaging system. The current characterization process, however, has been expanded to include characterization of non-CFRP fragments and shortly will begin characterization of fragments categorized as 3D.

The assessment, measurement, and the verification processes have been updated and are discussed in detail.

Assessment

After the fragment's associated panel information are entered into the DCS, the fragment's size category, material property, shape, and color are assessed. The fragments are categorized as 2D or 3D depending on which imaging system will be used to measure the fragment's physical size parameters (X_{DIM}, Y_{DIM}, Z_{DIM}, average cross-sectional area, and volume). Initially the categorization of a fragment as 2D and 3D was based on error analysis [2], however, with the improvements to the 2D imaging system and a detailed characterization of the 3D imaging systems, the size threshold was determined based on the performances of the imaging systems. The size threshold has been set at 3 mm; i.e., all fragments with a minimum dimension of 3 mm or greater are measured on the 3D imaging system and all other fragments will be measured on the 2D imaging system.

Once the fragments are organized into their respective size category (2D or 3D), their material property, shape, and color are assessed. The fragments are placed under a microscope such that the technicians can better inspect the fragment features. There are 13 material categories based on the materials used in the fabrication of DebriSat: aluminum, carbon fiber reinforced polymer

(CFRP), copper, epoxy, glass, Kapton tape, Kevlar, multi-layered insulation, printed circuit board (PCB), plastics, solar cells, silicone, stainless steel, and titanium. In addition to this list, a "metal" category was added to aid the technicians during the material assessment. There are three materials that fall under this "metal" category: aluminum, stainless steel, and titanium, due to their similar appearances. When the "metal" is selected, the material is later identified based on the density calculation from the mass and size measurements (this is one of the items the independent verifier examines during the certification process). To aid in the assessment of the fragment's material property, the fragments are compared to samples and pictures of each material type.

The number of shape categories remain the same at six, however, improvements were made in the definitions of each shape to help the technicians. The six shape categories are: (i) straight rod/needle/cylinder, (ii) bent rod/needle/cylinder, (iii) flat plate, (iv) bent plate, (v) nugget/parallelepiped/spheroid, and (vi) flexible. Several samples of each shape category are provided to the technicians to assist in the fragment shape assessment.

The color categories have been reduced by one to 13. Previously, the color category included a "burnt/charred" option, however, it has now been removed. The list and definitions of each shape and color category are explained in Ref. [2]. Once the assessments are completed on the fragments, the fragments are passed onto mass and size measurements.

As of the writing of this article (August 2017), there is a total of 19,314 fragments (all 2D) that have completed assessment. Out of these fragments, 17,098 fragments are assessed as CFRP, and 2,216 fragments are assessed as non-CFRP material.

Mass Measurement
Once the fragment assessments have been completed, the next step in the fragment characterization process is the measurement of its mass. Three mass balances that have been selected to perform the mass measurements: a BM-22, a PGL-203, and a CY-510. The three balances were selected based on their readability, sensitivity, and maximum capacity as shown in Table 7. The BM-22 is a microbalance that meets the measurement requirements and is capable of measuring DebriSat fragments that are very small. Due to its high sensitivity to the slightest disturbances, the microbalance was placed under a draft shroud on a granite table.

Table 7 Summary of mass balances used for mass measurement

Model	Capacity (g)	Readability (g)	Std. Dev. (g)
BM-22	5	0.000001	0.000004
PGL 203	200	0.001	0.002
CY-510	510	0.001	0.001

As the fragment mass measurements continued, it was determined that another microbalance was needed to increase the productivity. As a result, a second microbalance was acquired and incorporated to measure the fragment masses. Similar to the first microbalance, the second microbalance is placed under a draft shroud on a separate granite table. To date, approximately 17,000 fragments have been massed on one of the two microbalances (see Figure 5). The breakdown of the fragments that were massed on each microbalance are shown in Table 8, where the first and second microbalances are denoted as Micro 1 and Micro 2, respectively. As seen in Figure 5, the majority of the fragments that have been massed so far have very small mass. Table 9 shows that the average mass of the fragments massed to date is less than 250 milligrams. As the characterization continues, bigger fragments will be massed and the maximum and average mass measurements will change significantly from what is shown in Table 9.
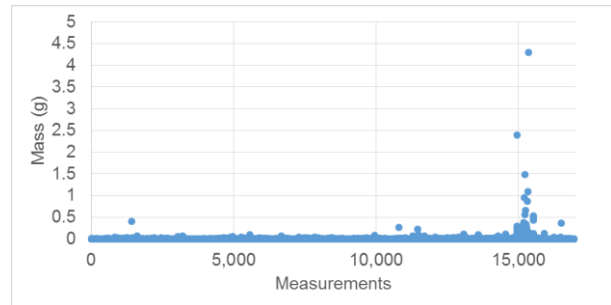

Figure 5 DebriSat fragment mass measurements as of August 2017

Table 8 Mass measurements as of August 2017

	Fragment count
Micro 1	11,686
Micro 2	5,243
Total massed	16,929

Table 9 Mass measurements of 17K fragments as of August 2017

Parameters	Masses (g)
Maximum	4.292788
Average	0.002431
Minimum	0.000001

Due to the sensitivity of the microbalance to environmental effects, the temperature and the humidity at the time of each mass measurement is also recorded and archived. A temperature and humidity sensor was placed within 2 m of each microbalance so that the temperature and humidity are also measured at the time of each mass measurement. The temperature and humidity measurements from the approximately 17,000 mass measurements are shown in Figure 6 and Figure 7,

respectively and a summary of that data are shown in Table 10. Both the temperature and humidity measurements are well within the acceptable working conditions of the balances. As the characterization efforts continue, larger fragments will be massed and will have their masses measured with the other two balances.

Table 10 Temperature and humidity measurements of 17K fragments

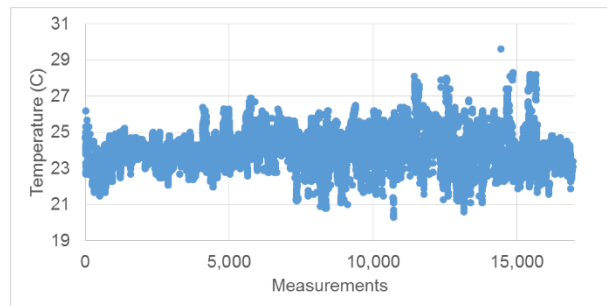| Parameters	Max	Average	Min
Temperature (C)	29.6	24.1	20.3
Humidity (%)	59.4	44.5	23.2

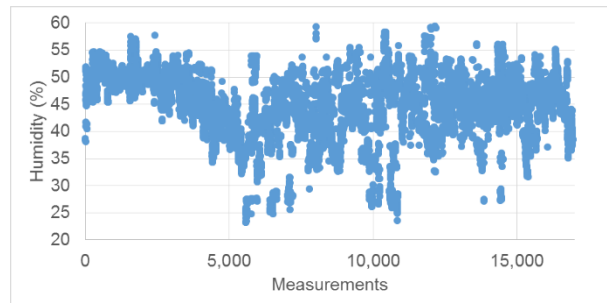Figure 6 Temperature measurements at each mass measurement

Figure 7 Humidity measurements at each mass measurement

Size Measurements

The next step in the characterization process is the determination of the fragment's size characteristics (L_C, average cross-sectional area, and volume). Based on the fragment's size categorization as either 2D or 3D, the fragments size characteristics are measured using either the 2D imaging system or the 3D imaging system. Both imaging systems utilize point-and-shoot cameras for fragment image acquisition[5]. The images are then processed to generate their fragment's size characteristics. The fragment size characteristics, images, and associated metadata (e.g., revision history, timestamps, etc.) generated during the measurement process are archived in the database.

The initial configuration of the 2D imaging system assumed negligible height (i.e., $Z_{DIM}=0$ since the CFRP fragments have negligible height) and only the fragment's two largest orthogonal in-plane dimensions (denoted as X_{DIM} and Y_{DIM}) were measured. However, as the characterization activities progressed and non-CFRP fragments were characterized, a right angle wedge mirror was incorporated to capture the height of the fragment. The in-plane dimensions X_{DIM} and Y_{DIM} are measured by processing the back light image (i.e., silhouette) and the height, Z_{DIM}, is obtained from the front lit image (see Figure 8).

Back light image   Front light image

Figure 8 Back lit and front lit images from updated 2D imaging system with mirror

There are two 2D imaging systems that have been developed and implemented to increase the productivity during fragment characterization process. To ensure that the characteristic length error requirement was being satisfied with the inclusion of the mirror to measure the third longest dimension, Z_{DIM}, two hollow disks were used to examine the characteristic length accuracies of both 2D imagers. The hollow disks have the same outer diameter and inner diameter and their only difference is the heights, 0.25 mm and 0.13 mm, respectively. Ten measurements were taken for each hollow disk and on each imager. The characteristic length (L_C) error was calculated by comparing the 2D imaging system measurements to the actual dimensions of the hollow disks. The hollow disk dimensions were physically measured using micrometers and their characteristic lengths were calculated. Table 11 shows the L_C accuracies of both hollow disks on the two 2D imaging systems with the mirror and without the mirror. The L_C accuracies are well within the ±10% requirement with and without the mirror, but the accuracies improve with the addition of the mirror. Therefore, all pre-mirror size measurements are acceptable and do not need to be repeated. Designations have been added to the database to identify pre- and post-mirror size characterized fragments.

Table 11 L_C accuracy of the two 2D imagers

Imager	Disk (mm)	Error without mirror (%)	Error with mirror (%)
1	0.25	-1.93	-1.22
1	0.13	-1.18	-0.90
2	0.25	-1.18	-0.55
2	0.13	-0.54	-0.26

To date, 13,885 2D fragments have completed assessment, mass, and size measurements. Out of these fragments, a little over 9,000 fragments had their sizes measured prior to the addition of mirror and the remaining fragments had their sizes with measured with the mirror setup. The distributions are shown in Table 12.

Table 12 Size measurements (2D) as of August 2017

	Fragment count
Pre-mirror setup	9,346
2D Imager 1	2,547
2D Imager 2	1,992
Total characterized	13,885

When fragments are categorized as 3D, their sizes are measured on the 3D imaging system. The 3D imaging system consists of a six-camera configuration with a turntable and studio lighting (to minimize shadowing). The 3D object on the turntable is reconstructed from multiple 2D images using a space-carving technique [6,7]. From the space-carved object, the representative 3D point cloud is generated and the characteristic length and volume are calculated. The average cross-sectional area is calculated as the average of the projected areas, where the projected areas are calculated based on the object silhouettes [8]. The fragment measurement data and their images are all archived in the DCS database. Currently, the performance of the 3D imaging system is being verified and once completed the system will be put in service. To date, no fragment size has been measured on the 3D imaging system.

To verify the performance of 3D imaging system, four shapes (a cone, a rectangular prism, a square pyramid, and a sphere) and three sizes for each shape (small, medium, and large) were characterized. The objects are shown in Figure 9 and their dimensions are provided in Table 13.
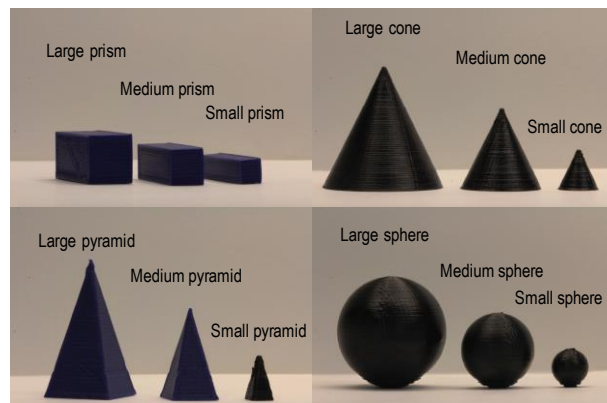

Figure 9 Objects used to characterize 3D imaging system

For each object, ten measurements were performed on the 3D imaging system. The L_C errors were calculated for each object by comparing the measured/computed values to their actual values. Table 14 shows that the L_C errors for each object are within the requirement.

Table 13 Object dimensions (in mm)

Shape	Large	Medium	Small
Prism	12.57 x 12.73 x 25.31	9.56 x 9.56 x 25.39	9.59 x 6.22 x 25.40
Cone	29.97 dia. x 29.76 height	19.92 dia. x 19.74 height	10.00 dia. x 9.71 height
Pyramid	15.22 x 15.23 x 29.31	10.15 x 10.11 x 19.33	4.99 x 4.97 x 9.38
Sphere	30.44 x 30.15 x 29.80	20.31 x 20.10 x 19.91	10.78 x 10.03 x 9.96

Table 14 L_C errors with 101 images

	Large	Medium	Small
Cone	-1.42%	-1.32%	-2.09%
Prism	-3.01%	-3.34%	-4.55%
Pyramid	-4.51%	-4.10%	-8.68%
Sphere	-1.44%	-2.35%	-2.69%

Verification

The final step in the characterization process and perhaps the most important is verification. The verification step involves a pass or fail logic to analyze and confirm all the appropriate data for each fragment are stored in the DCS database. Verifying the debris fragments requires careful attention to detail and knowledge of the entire DebriSat characterization process. The technicians analyze the fragment data starting with the panel identification and chamber location and checks if the corresponding panel information is correct. The next step involves checking the fragment's material, shape, and color under a microscope and compares them to the information in the database. Next, the mass measurement and size measurements in database are compared to the fragment. If there are any inconsistencies in the measurements, the verification fails. The final step is to check that all images and the point cloud files are present and correct. If any of the images are absent or incorrect, the fragment fails verification and must be re-characterized. To ensure accurate results, the verifying technician cannot previously be associated with the fragment. Once the fragments complete verification no further modifications are possible.

During each characterization activity, the processing times were examined. Table 15 shows the processing times for assessment, mass and size (2D) measurements, and verification; specifically, the average time per fragment is determined based on the number of fragments

examined. The number of fragments that were used to calculate the average time per fragment differs from the total number of processed fragments since the time information was not captured for all the processed fragments. On average, the assessment (2D/3D, material, shape, and color) takes around 5.5 minutes per fragment, which includes the setup as well (i.e., removing the fragment from its storage bag and placing it under the microscope). For mass measurement, it takes around 6.3 minutes per fragment to measure the mass, measure the temperature and humidity, and to archive the data in the DCS database. This average time includes the initial waiting period for the microbalances to adapt to the environment as well as weighing the fragments. The average time to measure the fragment size on the 2D imaging system is around 7.1 minutes. This time includes the setup of the equipment as well as the measurement and uploading to the database. The average time for the size measurement is higher than the assessment and mass measurements since the data size uploaded to the DCS from the 2D imaging system is much larger due to images. The average time to verify the fragment data in the DCS database is around 6.2 minutes. The average times per fragment will continue to be examined to identify where improvements can be made to increase productivity.

Table 15 Average characterization time per fragment

	Fragment count	Average time per fragment (minutes)
Assessment	2,694	5.5
Mass measurement	16,929	6.3
Size measurement (2D)	8,298	7.1
Verification	743	6.2

To date, a total of 2,842 fragments have been verified and two Gage R&R tests [9,10,11] have been conducted to assess the repeatability and reproducibility of the processes and devices used in the characterization process. The results from the Gage R&R tests are discussed in Section III.

III. GAGE REPEATABILITY AND REPRODUCBILITY TEST

Gage repeatability and reproducibility (Gage R&R) test is a tool commonly used to quantify the amount of variation in a measurement system and the sources of the variations [9,10,11]. Repeatability measures the contribution to the gage variance when the same part is measured multiple times with all other factors held constant. Reproducibility gives contribution to the gage variance from additional factors, in this case, the operators. In order to deem a measurement system acceptable, the total variation must be below 10% and for conditional acceptance below 30%. The measurement system is unacceptable when the total variation is greater than 30%.

The components that effect variability are repeatability and reproducibility. Repeatability is an indicator for variability from the equipment; in the current case this includes both microbalances and the 2D imaging systems. Reproducibility is an indicator to whether or not the characterization process and procedure carried out by technicians are good. The total Gage R&R is computed as the root-mean-square of the repeatability and reproducibility. The analysis of these varying factors is important for showing the procedures are developed in a way that can be utilized by any operator. As such, the Gage R&R tests are conducted for every 1,000 fragments that pass verification and to ensure integrity of data by a random selection of five fragments and three experienced technicians. The study utilizes Minitab software [10] to compare measurements taken during the testing to the original database entry.

To carry out the Gage R&R test, three technicians with characterization experience were randomly selected. The test started with both micro mass balances and concluded with the 2D imagers. The assessments were not included in the study because the assessment data are qualitative with no equipment used. First, each of the technicians took the mass of five CFRP flat plate fragments at random with each mass balance. For each fragment, the mass measurements taken by the technicians and the mass measurement stored in the DCS database were analyzed. Next, the same five fragments were imaged by the same three technicians on both 2D imaging systems to measure the fragments sizes. For each fragment, the size measurements taken by the technicians and the size measurement stored in the DCS database were analyzed. All the data from mass measurements and size measurements were analyzed using Minitab's expanded Gage R&R tool.

III.I Gage R&R Test 1

The first test was conducted after the first 1,000 DebriSat fragments were verified and the second test after the second 1,000 DebriSat fragments were verified. For both tests, five CFRP flat plates were selected at random and the masses and sizes were measured. CFRP flat plate fragments were chosen instead of needle-like simply because they are sturdier and would survive the significant amount of handling during the test.

Mass Measurement Results

The first Gage R&R test took place over a period of two days due to ensuring the process was correct. All of the mass measurements were taken during the first day and the results are shown in Table 16, Figures 9 and 10. Table 16 and Figure 10 shows the variations that were calculated based on the mass measurements and Figure 10 shows the variations between technicians (including

the data from DCS denoted as Technician 4) for each fragment. The total Gage R&R was 7.3%, which is in the acceptable range for the test criteria. The variations are coming from the equipment rather than the technicians and the procedure. The part-to-part variation examines the differences between the test articles and a high variation suggests that each gage is able to distinguish each part that is tested is different. Figure 11 shows that the variations in mass measurements of each fragment by the technicians are very low and that the mass measurement processes are very good.

Table 16 Test 1: Calculated mass measurement variations

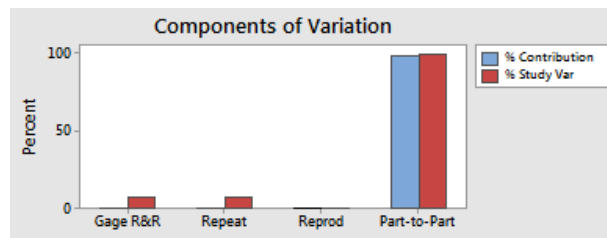|	Mass variation (%)
Repeatability	7.30
Reproducibility	0.00
Total Gage R&R	7.30

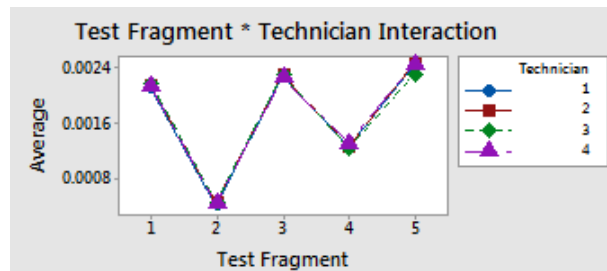Figure 10 Test 1: Components of variation mass measurements

Figure 11 Test 1: Mass measurement variations between technicians for each fragment

Size Measurement Results

The size measurements of the five fragments were taken on the second day of the first Gage R&R test. The measurements were taken on both 2D imaging systems and the results were analyzed with the size data in the DCS database. There are three dimensions associated with each size measurement, X_{DIM}, Y_{DIM}, and Z_{DIM} corresponding to the three largest orthogonal dimensions, therefore, the Gage R&R were analyzed for each dimension. Table 17 shows the variations for each dimension X_{DIM}, Y_{DIM}, and Z_{DIM}, respectively. Similar to the results from the mass measurements, the variations due to reproducibility is low, indicating that the procedures developed for the measurements are both

very good. The variations are mainly from the equipment and not the technicians. The Gage R&R for the X_{DIM} and Y_{DIM} are very low with 11.25% and 5.77%, respectively, however, the Gage R&R for the Z_{DIM} is 54.46% which surpasses the acceptable range and is in the unacceptable range. An explanation for the significant Gage R&R for the Z_{DIM} is the Z_{DIM} measurements taken by the technicians during the tests were determined using the mirror, however, the Z_{DIM} data from the DCS was calculated and derived based on mass and density. In fact, this large Gage R&R value is a positive result because it detected the process change.

Table 17 Test 1: Calculated size measurement variations

Variations	X_{DIM} (%)	Y_{DIM} (%)	Z_{DIM} (%)
Repeatability	9.01	5.56	36.26
Reproducibility	6.73	1.54	40.64
Total Gage R&R	11.25	5.77	54.46

Gage R&R Test 1 Results

The Gage R&R results from both the mass and size measurement tests showed that the measurement systems and the processes are acceptable. However, the measurements were averaged between the two balances and two 2D imaging systems rather than examining the variations for each equipment independently. Therefore, the procedure was updated to examine the equipment variation individually. These independent tests were performed in the second Gage R&R test.

III.II Gage R&R Test 2

The second test was conducted after the second 1,000 DebriSat fragments were verified. The procedures for performing the Gage R&R tests were updated to examine the equipment variation individually rather than the two microbalances as one equipment and the two 2D imaging systems as one equipment.

Mass Measurement Results

Three technicians measured masses of five fragments in random order for each microbalance. The mass measurements were compared to those on the DCS database and the Gage R&R were examined. Table 18 shows the Gage R&R analyses for microbalance 1 and microbalance 2. Both Gage R&R are very low with 7.28% for microbalance 1 and 5.25% for microbalance 2. In addition, the variations are due to repeatability, or equipment, and not by the reproducibility, or technicians and procedure.

Table 18 Test 2: Calculated mass measurement variations

Variations	Mass micro 1 (%)	Mass micro 2 (%)
Repeatability	7.28	5.25
Reproducibility	0.00	0.00
Total Gage R&R	7.28	5.25

Size Measurement Results

Next, the same five fragments were moved to the 2D imaging systems and their sizes were measured once on each system by three technicians. The measurements and the measurements from the DCS were analyzed to calculate the Gage R&R. The results from both 2D imaging systems are shown in Table 19 and Table 20, where Table 19 shows the variations of 2D imager 1 and Table 20 shows variations of 2D imager 2. The Gage R&R for X_{DIM} on both 2D imagers were in the acceptable range, however, the variations of Y_{DIM} on both 2D imagers were concerning. Further investigations are ongoing to identify the source(s) of the variations. The variations in Z_{DIM} are high since two calculations of Z_{DIM} are compared, one calculation is with the height determined from the mirror image and the other calculation was derived based on the fragment's mass and density.

Table 19 Test 2: Calculated size measurement variations 2D imager 1

Variations	X_{DIM} (%)	Y_{DIM} (%)	Z_{DIM} (%)
Repeatability	13.00	16.60	61.74
Reproducibility	0.00	13.76	59.72
Total Gage R&R	13.00	21.56	85.90

Table 20 Test 2: Calculated size measurement variations 2D imager 2

Variations	X_{DIM} (%)	Y_{DIM} (%)	Z_{DIM} (%)
Repeatability	9.67	17.44	76.73
Reproducibility	6.44	13.89	36.34
Total Gage R&R	11.62	22.30	84.90

Gage R&R Test 2 Results

After 2,000 DebriSat fragments were verified, the second Gage R&R test was conducted to examine the equipment and procedure variabilities. The second test was conducted and analyzed such that the microbalances and the 2D imaging systems were examined individually rather than treating the two microbalances as one piece of equipment and the two 2D imaging systems also as one piece of equipment. Similar to the first test, the variations from the mass measurements on both microbalances are low, indicating that the equipment as well as the procedures are very good. In contrast, the size measurements on 2D imaging systems were of concern, specifically, the variations in Y_{DIM} were much higher than the variations in X_{DIM} (on both 2D imagers). While the Y_{DIM} measurements are dependent on X_{DIM}, the source of the variation was not conclusively determined. Further investigations are ongoing to identify the root cause(s) of the variations to determine if the equipment and/or the procedure needs to be updated and improved.

IV. CONCLUSION AND FUTURE

Rigorous procedures for each activity in the post-impact phase of the DebriSat project has matured to improve efficiencies as well as to incorporate new processes/equipment based on lessons learned. Furthermore, the procedures have been developed and updated to be independent of technicians to adapt to growing and ever changing group of technicians. One of the biggest challenge is handling and working with fragments in the 2 mm range, and the technicians have focused on extreme care and attention during each activity. A verification step has been implemented in order to mitigate inaccuracies in the information stored in the database and to ensure the integrity of the data archived for each fragment.

There has been a steady increase in the panel preparation for X-ray imaging and object detection and completed all the panels that are greater than 2/3 of the original size. The remaining foam panels are all broken panels, thus, a procedure has been developed and is currently being verified to process the broken panels. As the third year of post-impact processing continues, the majority of the focus has been on fragment extraction and characterization. Over 20,000 fragments have been collected through extraction, and over 13,000 fragments have been characterized. In addition, close to 3,000 fragments have been verified. While only fragments that qualify as 2D are characterized to date, the 3D fragments are beginning to be characterized.

V. ACKNOWLEDGEMENTS

VI. REFERENCES

[1] Rivero, M., Kleespies, J., Patankar, K., Fitz-Coy, N., Liou, J.-C., Sorge, M., Huynh, T., Opiela, J., Krisko, P., and Cowardin, H., "Characterization of Debris from the DebriSat Hypervelocity Test," Proceedings of the 66th International Astronautical Congress, IAC-15-A6.2.9x30343, Jerusalem, Israel, October 2015.

[2] Rivero, M., Shiotani, B., Carrasquilla, M., Fitz-Coy, N., Liou, J.-C., Sorge, M., Huynh, T., Opiela, J., Krisko, P., and Cowardin, H., "DebriSat Fragment Characterization System and Processing Status," Proceedings of the 67th International Astronautical Congress, IAC-16-A6.2.8x35593, Guadalajara, Mexico, September 2016.

[3] Kleespies, J., and Fitz-Coy, N., "Big Impacts and Big Data: Addressing the Challenges of Managing

DebriSat's Characterization Data," Proceedings of the 2016 IEEE Aerospace Conference, Big Sky, MT, USA, March 5-12, 2016.

[4] Kleespies, J., and Fitz-Coy, N., "An Update on DebriSat's Debris Categorization System," Proceedings of the 67th International Astronautical Congress, IAC-16-A6.3.5x35674, Guadalajara, Mexico, September 2016.

[5] Shiotani, B., and Fitz-Coy N., "Imaging Systems for Size Measurements of DebriSat Fragments," Proceedings of the 68th International Astronautical Congress, IAC-17-A6.IP.41x39844, Adelaide, Australia, September 2017.

[6] K. N. Kutulakos and S. M. Seitz, "A Theory of Shape by Space Carving," in *The Proceedings of the Seventh IEEE International Conference on Computer Vision*, Kerkyra, Greece, 1999.

[7] A. Fitzgibbon, G. Cross and A. Zisserman, "Automatic 3D Model Construction for Turn-Table Sequences," in *3D Structure from Multiple Images of Large-Scale Environments, European Workshop*, Freiburg, Germany, 1998.

[8] T. Scruggs, "Average Cross-Sectional Area Calculation of DebriSat Fragments," University of Florida, Gainesville, FL, USA, 2017.

[9] Burdick RK, Borror CM, Montgomery DC, Books24x7 I. "Design and Analysis of Gauge R&R Studies: Making Decisions with Confidence Intervals in Random and Mixed ANOVA Models." Philadelphia, Pa; Alexandria, Va;: Society for Industrial Applied Mathematics; 2005.

[10] "What is a gage R&R (repeatability and reproducibility) study?" Minitab 17 Support . N.p., n.d. Website, http://support.minitab.com/en-us/minitab/17/topic-library/quality-tools/measurement-system-analysis/gage-r-r-analyses/what-is-a-gage-r-r-study/, [last visited July, 2016].

[11] "How to Perform a Gauge R and R Study." Adaptive Business Management Systems, n.d. Website, <https://adaptivebms.com/Explanation_of_Gauge_R_and_R_MSA/>. [last visited June 2016].